

# Comb Reference Signal Pattern Design for Integrated Communication and Sensing

Rui Zhang  
Department of Electrical  
Engineering  
University at Buffalo  
Buffalo, NY, USA  
[rzhang45@buffalo.edu](mailto:rzhang45@buffalo.edu)

Shawn Tsai  
Advanced Comm. Technology  
Comm. System Design  
MediaTek USA Inc.  
San Diego, CA, USA  
[shawn.tsai@mediatek.com](mailto:shawn.tsai@mediatek.com)

Tzu-Han Chou  
Advanced Comm. Technology  
Comm. System Design  
MediaTek USA Inc.  
San Diego, CA, USA  
[tzuhan.chou@mediatek.com](mailto:tzuhan.chou@mediatek.com)

Jiaying Ren  
Advanced Comm. Technology  
Comm. System Design  
MediaTek USA Inc.  
San Diego, CA, USA  
[jiaying.ren@mediatek.com](mailto:jiaying.ren@mediatek.com)

**Abstract**—Ambiguity performances of reference signal patterns for integrated communication and sensing are studied via time delay and Doppler shift detection. A reference signal pattern with a staggering offset of a linear slope relatively prime to the transmission comb is suggested for low-complexity, standard-resolution sensing algorithms. We also propose an extended guard interval design to extend the maximum time delay for post-FFT sensing algorithms.

**Keywords**—Integrated communication and sensing, reference signal, 6G, delay and sum, 2D FFT

## I. INTRODUCTION

Recently, integrated communication and sensing (ICAS) has been envisioned to support diverse applications, such as activity or object detection, recognition, and tracking, potentially in the fifth generation advanced (5G-A) and the sixth generation (6G) era [1]. The integration of communication and sensing makes them mutually benefit and saves system resources. One of the research directions is communication centric ICAS, which realizes sensing functionality in a system primarily designed for communications. In such a system, sensing function can share communication reference signals (RS) and waveforms with current wireless systems, where orthogonal frequency division multiplexing (OFDM) has been adopted by 5G New Radio (NR), and extensively studied for radar sensing in vehicular applications to detect both Doppler shift and time delay [2-5]. For bistatic sensing where data payload is not known a priori, RS is the most straightforward radio resource for sensing receivers to estimate time delays and Doppler shifts caused by detectable targets. A feasibility study of leveraging 5G positioning reference signal (PRS) to radar sensing and positioning was presented in [6]. 5G PRS was optimized for delay estimation with a special design in the staggering offset sequence. However, the current 5G PRS is not specifically designed for both delay and Doppler estimation. Thus, improving the current 5G RS for both is critical for ICAS system. In this paper, with delay and sum [7] as well as 2D FFT [8] algorithms, we investigate PRS-like RS pattern for radar sensing and propose a new design for improved ambiguity performance. We also introduce an extended guard interval design for comb RS to enable inter-symbol-interference (ISI) removal beyond cyclic prefix (CP) duration for sensing.

## II. GENERAL COMB RS PATTERNS WITH UNIFORM SYMBOL SPACING

There are a few types of 5G NR RS: demodulation RS (DMRS), channel state information RS (CSI-RS), tracking RS

(TRS), phase tracking RS (PTRS), and positioning RS (PRS) [9]. They can be generalized by the RS pattern as shown in Fig. 1. Let  $S_{sub}$  (unit in subcarrier numbers) be the RS frequency domain spacing of resource elements (REs) (is also called transmission comb) and  $S_{sub} \geq 2$  for comb structure,  $S_{sym}$  (unit in symbol numbers) the time domain separation of the RS symbols,  $F_i$  (unit in subcarrier numbers) the frequency domain RE offset (or the staggering offset) of the  $i$ -th RS symbol. The RS patterns can be tuned by  $S_{sub}$ ,  $S_{sym}$  and  $F_i$ . In this paper, we will focus on analyzing such a comb structure of uniform RE/symbol spacing with staggering frequency offsets.

This comb structure has several benefits. First, it boosts energy per RE for better coverage, compared to pure time-domain multiplexing (TDM) of OFDM symbols. Second, it maximizes the delay resolution an OFDM symbol can offer due to its span across the entire channel bandwidth, compared to subband contiguous-RE-block FDM. Third, it enables either different base-station PRS multiplexing or data RE insertion. However, the comb structure introduces delay ambiguity. Therefore, the RS pattern with multiple comb RS symbols with a cycle of staggering offsets within the coherent processing interval (CPI) is adopted in 5G PRS to preserve the maximum unambiguous delay up to one effective OFDM symbol length. For consecutive two OFDM symbols, staggering offsets are paired one-half-comb-size ( $S_{sub}/2$ ) apart. Also, if more OFDM symbols can be allocated, offsets further sweep over full  $S_{sub}$  REs to cover the entire frequency range, e.g., two pairs of stagger offsets (0, 2) and (1, 3) in the case of  $S_{sub} = 4$  comb. The design was considered for scenarios where PRS resource may not be available for more than two symbols within the coherent processing interval. Such paired one-half-comb-size-apart staggering offsets extend detectable delay range.

However, extra aspects derived from general sensing require another look at other possible RS patterns. Specifically, with Doppler shift added to the estimated variables, ambiguities arise in the two-dimensional delay-and-Doppler plane. Under a fixed number of REs, increasing  $S_{sub}$  and  $S_{sym}$  can increase the occupied bandwidth and the time duration, which enhances the range (delay) resolution and the velocity (Doppler) resolution, respectively. Such resolution improvement by tuning  $S_{sub}$  and  $S_{sym}$ , however, comes with the cost of worse maximum unambiguous delay and Doppler. In the following sections, we

will investigate the ambiguity performance of different staggered RS patterns using different sensing algorithms. Examples of RS patterns with uniform symbol spacing are listed below.

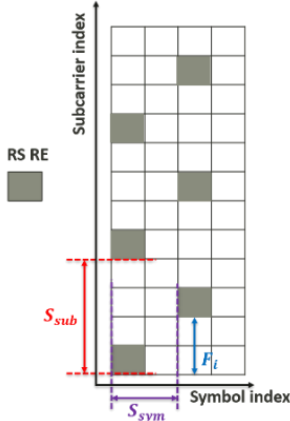


Figure 1. Illustration of general comb RS pattern.

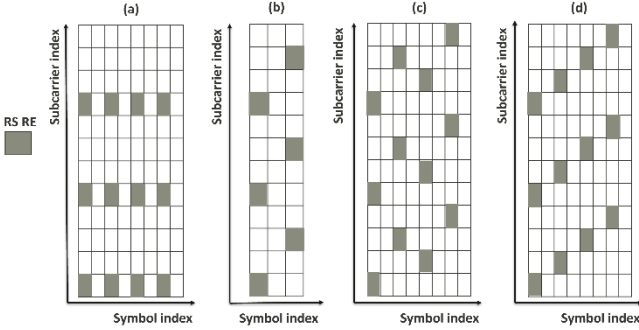


Figure 2. Instances of RS patterns.

#### A. Patterns similar to 5G PDCCH DMRS or TRS-like CSI-RS

This pattern keeps the same RE locations across all RS symbols. That is,  $F_i = F_j = \text{constant}$  for any  $i$ -th and  $j$ -th symbols. Fig. 2(a) represents the case of  $S_{sub} = 4, S_{sym} = 2$ .

#### B. Patterns similar to partial PRS (subgroup of full PRS staggering cycle)

In 5G PRS, partial PRS has the format of staggering two RS symbols' REs by half the comb size when  $S_{sub}$  is even, (i.e.,  $F_1 = f, F_2 = F_1 + S_{sub}/2$ , where  $0 \leq f < S_{sub}/2$ ). Fig. 2(b) depicts the comb-4 partial PRS with  $S_{sub} = 4, S_{sym} = 2$ .

#### C. Patterns with staggering offset similar to 5G PRS

Such RS patterns have the same staggering offset (with permutation) as that of 5G PRS. When  $S_{sym} = 1$ , the RS pattern is the same as 5G PRS. Fig. 2(c) illustrates an instance with  $S_{sub} = 4, S_{sym} = 2$ .

#### D. Proposed relatively-prime-to-comb-size linear-slope staggering scheme

In this paper, we propose a form of staggering offset such that  $F_i = \text{mod}(p \cdot (i - 1) + \beta_1, S_{sub})$ , where  $p$  is relatively prime to  $S_{sub}$  and  $\beta_1 \in \{0, 1, \dots, S_{sub} - 1\}$ ,  $i = 0, \dots, S_{sub} - 1$ . Fig. 2(d) shows an instance with  $S_{sub} = 4, S_{sym} = 2, p = 1$ , and  $\beta_1 = 0$ .

### III. AMBIGUITY FUNCTION OF DELAY AND SUM

The ambiguity function (AF) of a time sequence  $s(t)$  based on delay and sum is expressed as [7]

$$A(\tau, f_d) = \frac{1}{E_s} \left| \int_{-\infty}^{\infty} s(t) e^{j2\pi f_d t} s^*(t - \tau) dt \right|, \quad (1)$$

and  $E_s = \int_{-\infty}^{\infty} s(t) s^*(t) dt$ ,  $f_d$  is the Doppler frequency shift,  $\tau$  is the time delay. Let  $T_s$  be the effective OFDM symbol duration (the reciprocal of the subcarrier spacing (SCS)),  $T_{cp}$  be the CP duration,  $T = T_{cp} + T_s$  be the CP-added OFDM symbol duration,  $\mathbf{X}_i$  be the frequency-domain RE scrambling sequence of the  $i$ -th comb RS with a length of  $N$ . Assuming the Doppler shift is sufficiently small compared to OFDM base frequency, i.e.,  $|f_d| < f_{max}$  (where  $f_{max}$  is typically 1/10 of SCS), we can approximate that it only introduces a constant phase rotation over time-domain samples within an OFDM symbol. Recall that, for comb- $S_{sub}$  structure, the time sequence of the  $i$ -th OFDM RS symbol after IFFT is  $\mathbf{Y}$  of length  $N$ . Note that the  $n$ -th sample of time sequence  $\mathbf{Y}$  is

$$Y(n) = \sum_{k=0}^{S_{sub}-1} X_i(kS_{sub} + F_i) e^{j \frac{2\pi(kS_{sub} + F_i)n}{N}}, \quad (2)$$

where  $n = 0, 1, \dots, N - 1$ . One can further write

$$\begin{aligned} Y\left(n + \frac{Ni}{S_{sub}}\right) &= Y(n) e^{j \frac{2\pi F_i n}{S_{sub}}} \\ &= \sum_{k=0}^{S_{sub}-1} X_i(kS_{sub} + F_i) e^{j \frac{2\pi(kS_{sub} + F_i)(n + \frac{Ni}{S_{sub}})}{N}} \end{aligned} \quad (3)$$

where  $n = 0, 1, 2, \dots, N/S_{sub} - 1$  and  $i = 0, 1, 2, \dots, S_{sub} - 1$ .  $\mathbf{Y}$  can be further equally divided into  $S_{sub}$  subsets, where the  $h$ -th subset is  $\mathbf{Y}_h$  with a length of  $N/S_{sub}$  and has the following properties:

$$\mathbf{Y}_h = \mathbf{Y}_1 e^{j \frac{2\pi F_i h}{S_{sub}}}, \mathbf{Y}_h = \{Y(n)\}, n \in \left[ \frac{(h-1)N}{S_{sub}}, \frac{hN}{S_{sub}} \right] \quad (4)$$

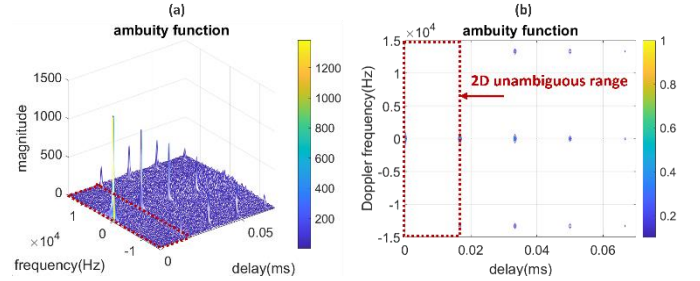


Figure 3. AF in the case of ( $S_{sub} = 4, S_{sym} = 1, F_i = F_j = 0$ ).

Let the transmitted time sequence of one CP-added OFDM symbol be  $\mathbf{Z}$  of length  $N' = (N + N_{cp})$ , and the  $n$ -th sample of time sequence  $\mathbf{Z}$  be

$$Z(n) = \sum_{k=0}^{S_{sub}-1} X_i(kS_{sub} + F_i) e^{j \frac{2\pi(kS_{sub} + F_i)(N - N_{cp} + n)}{N}}, \quad (5)$$

where  $n = 0, 1, \dots, N' - 1$ . As time samples of one OFDM symbol are divided into  $S_{sub}$  subsets that are repetitive with piecewise phase rotation in Eq. (4), correlation peaks of delay-

and-sum always happen at  $\tau = T_s l / S_{sub} = Nl / S_{sub} \cdot (T_s / N)$ , where  $Nl / S_{sub}$  is the index of OFDM discrete-time samples at  $l = 0, 1, \dots, S_{sub}$ . Let  $M$  be the number of RS symbols, the AF at time delay  $T_s l / S_{sub}$  and Doppler frequency  $f_D$  is expressed as:

$$A\left(\frac{T_s l}{S_{sub}}, f_D\right) = \left| \sum_{m=0}^{M-1} \sum_{n=mS_{sym}N' + \frac{Nl}{S_{sub}}}^{mS_{sym}N' + N' - 1} Z(n)Z^*\left(n - \frac{Nl}{S_{sub}}\right) e^{\frac{j2\pi f_D n T}{N}} \right|. \quad (6)$$

Assuming  $X_i$  preserves constant envelope in the time domain (e.g., frequency domain Zadoff-Chu sequence), we obtain

$$\begin{aligned} A\left(\frac{T_s l}{S_{sub}}, f_D\right) &= \left| \sum_{m=0}^{M-1} e^{\frac{j2\pi F_m l}{S_{sub}}} \sum_{n=mS_{sym}N'}^{mS_{sym}N' + N' - 1 - \frac{Nl}{S_{sub}}} Z(n)Z^*(n) e^{\frac{j2\pi f_D (n + \frac{Nl}{S_{sub}}) T}{N}} \right| \\ &= \left| S \cdot e^{\frac{j2\pi f_D l T}{S_{sub}}} \sum_{m=0}^{M-1} e^{\frac{j2\pi F_m l}{S_{sub}}} \sum_{n=mS_{sym}N'}^{mS_{sym}N' + N' - 1 - \frac{Nl}{S_{sub}}} e^{\frac{j2\pi f_D n T}{N}} \right|, \end{aligned} \quad (7)$$

where  $S = Z(n)Z^*(n)$  is a constant. In the case of  $f_D = z_1 N / T$ ,  $z_1 \in \mathbb{Z}$ , (e.g.,  $f_D = 0$ ), the staggering patterns  $\{F_m\}$  directly affects the locations of the side peaks by

$$A\left(\frac{T_s l}{S_{sub}}, f_D\right) = \left| S \cdot \left(N' - \frac{Nl}{S_{sub}}\right) \sum_{m=0}^{M-1} e^{\frac{j2\pi F_m l}{S_{sub}}} \right|, \quad (8)$$

For instance,  $M = S_{sub}$ ,  $\{F_m\}_{m=0}^{S_{sub}-1} = \{0, 1, \dots, S_{sub} - 1\}$ , the side peaks within the time delay range  $(0, T_s)$  can be eliminated as  $\sum_{m=0}^{k-1} e^{\frac{j2\pi F_m l}{S_{sub}}} = 0$  for  $l = 1, \dots, S_{sub} - 1$ . Delay and sum algorithm requires the time sequences derived from  $X_i$  to have desirable autocorrelation and partial correlation properties. Characteristics of AF derived from delay-and-sum algorithm over various RS patterns in Section II will be examined next.

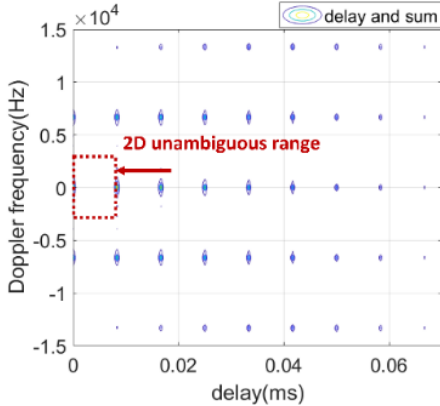


Figure 4. AF in the case of  $(S_{sub} = 8, S_{sym} = 2, F_i = F_j = 0)$ .

#### A. Patterns similar to 5G PDCCH DMRS or TRS-like CSI-RS

For RS patterns without staggering in Section II. A, based on Eq. (7) and Eq. (8), the peak locations in the 2D AF beside the true delay and Doppler frequency are  $(\tau + lT_s / S_{sub}, f + k / S_{sym}T)$ , where  $l \in \mathbb{Z}$ ,  $0 \leq l \leq S_{sub}$ , and  $k \in \mathbb{Z}$ ,  $-S_{sym} \leq k \leq S_{sym}$ , with the exception of  $(\tau, f \pm 1/T)$ . Fig. 3 shows an

instance with  $S_{sub} = 4$ ,  $S_{sym} = 1$ ,  $F_i = F_j = 0$ , and  $SCS = 15$  kHz. Fig. 3(b), which will be used for ambiguity performance analysis, is the contour of Fig. 3(a). The 2D maximum unambiguous range, as shown in the red squared area in Fig. 3(b), designates maxima of unambiguous time delay and Doppler frequency in the 2D AF variable domain. As shown in Fig. 3(b), arbitrary mainlobes with associated side peaks fall outside the red square, meaning no ambiguities exist in the designated 2D maximum unambiguous range. Furthermore, Fig. 4 shows another example with  $S_{sub} = 8$ ,  $S_{sym} = 2$ , and  $F_i = F_j = 0$ . Note that the 2D maximum unambiguous range is not unique. Depending on application scenarios, the designated 2D maximum unambiguous range around the true delay and Doppler  $(0,0)$  could have different options:

- 1) In the case of  $S_{sym} > 1$ , time delay is from 0 to  $T_s / S_{sub}$ , and Doppler frequency from  $l$  to  $l + 1 / S_{sym}T$ , where  $l$  is a specified value with  $-1 / S_{sym}T \leq l \leq 0$ .
- 2) In the case of  $S_{sym} = 1$ , time delay is from 0 to  $T_s / S_{sub}$ , Doppler frequency from  $l$  to  $l + N / S_{sym}T$ , where  $l$  is a specified value with  $-N / S_{sym}T \leq l \leq 0$ .

However, the maximum unambiguous delay in this case is always restricted to  $T_s / S_{sub}$ .

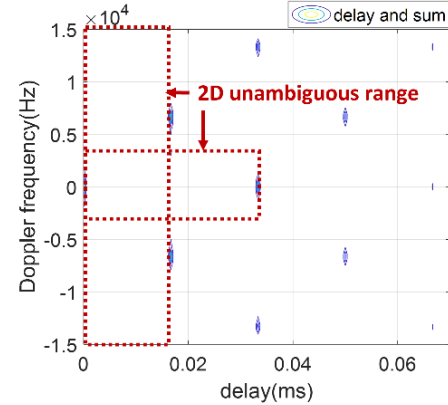


Figure 5. AF in the case of  $(S_{sub} = 4, S_{sym} = 1, \text{partial PRS})$ .

#### B. Patterns similar to partial PRS

In this case, for even integer  $l_1$ , the side peak locations are  $(\tau + l_1 T_s / S_{sub}, f + k / S_{sym}T)$  in the 2D AF, where  $0 \leq l_1 \leq S_{sub}$ , and  $k \in \mathbb{Z}$ ,  $-S_{sym} \leq k \leq S_{sym}$ , with the exception of  $(\tau, f \pm 1/T)$ , where  $(\tau, f)$  is true delay and Doppler. For odd integer  $l_2$ , the side peak locations are  $(\tau + l_2 T_s / S_{sub}, f + (1/2 + k) / S_{sym}T)$  in the 2D AF, where  $0 \leq l_2 \leq S_{sub}$  and  $k \in \mathbb{Z}$ ,  $-S_{sym} \leq k \leq S_{sym}$ . Fig. 5 shows an example of  $S_{sub} = 4$ ,  $S_{sym} = 1$ , and  $F_1 = 0, F_2 = 2$ . Such RS patterns (half-comb-size staggering) can extend the maximum unambiguous delay from  $T_s / S_{sub}$  of no staggering to  $2 \cdot (T_s / S_{sub})$ . Depending on application scenarios, the designated maximum unambiguous 2-D range around the true delay and Doppler frequency pair  $(0,0)$  could have following options:

- 1) Comb-sized fractional-symbol delay unambiguity:
  - a. In the case of  $S_{sym} > 1$ , time delay is from 0 to  $T_s / S_{sub}$ , and Doppler from  $l$  to  $l + 1 / S_{sym}T$ , where  $l$  is a specified value with  $-1 / S_{sym}T \leq l \leq 0$ .

- b. In the case of  $S_{sym} = 1$ , time delay is from 0 to  $T/S_{sub}$ , and Doppler from  $I$  to  $I + N/S_{sym}T$ , where  $I$  is a specified value with  $-N/S_{sym}T \leq I \leq 0$ .
- 2) Extended maximum unambiguous delay: time delay is from 0 to  $2T_s/S_{sub}$ , and Doppler range is now from  $J$  to  $J + 1/(2S_{sym}T)$ , where  $J$  can be specified within the range of  $-1/(2S_{sym}T) \leq J \leq 0$ , as shown by the horizontally wider dotted red rectangle of Fig. 5.

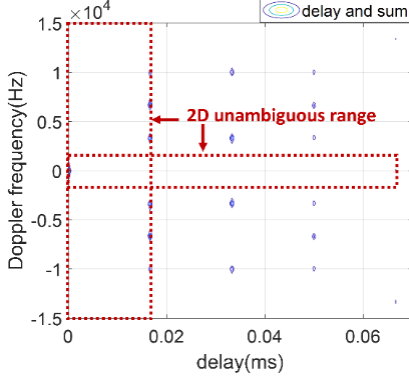


Figure 6. AF in the case of ( $S_{sub} = 4, S_{sym} = 1$ , PRS like pattern).

### C. Patterns with staggering offset similar to 5G PRS

Fig. 6 shows an instance of PRS pattern with  $S_{sub} = 4$ ,  $S_{sym} = 1$  and  $\{F_0, F_1, F_2, F_3\} = \{0, 2, 1, 3\}$ . As one can observe, the PRS pattern can extend the maximum unambiguous delay to  $T_s$  at the cost of smaller Doppler unambiguity. Based on Eq. (8) and depending on application scenarios, 2D maximum unambiguous range around the true delay and Doppler (0,0) have following options.

- 1) Comb-sized fractional-symbol delay unambiguity:
  - a. In the case of  $S_{sym} > 1$ , time delay is from 0 to  $T_s/S_{sub}$ , and Doppler from  $I$  to  $I + 1/S_{sym}T$ , where  $I$  is a specified value with  $-1/S_{sym}T \leq I \leq 0$ .
  - b. In the case of  $S_{sym} = 1$ , time delay is from 0 to  $T/S_{sub}$ , and Doppler from  $I$  to  $I + N/S_{sym}T$ , where  $I$  is a specified value with  $-N/S_{sym}T \leq I \leq 0$ .
- 2) Full-symbol unambiguous delay extended to  $T_s$ : Doppler range is now from  $J$  to  $J + 1/S_{sym}S_{sub}T$ , where  $J$  can be specified within the range of  $-1/S_{sym}S_{sub}T \leq J \leq 0$ , as shown by the horizontally wider dotted red rectangle of Fig. 6.

### D. Comb-size-relative-prime linear-slope staggering scheme

In this case, side peak locations are  $(\tau + lT_s/S_{sub}, f + p \cdot l/S_{sub}S_{sym}T + k/S_{sym}T)$  in the 2D ambiguity functions, where  $0 \leq l \leq S_{sub}$ , and  $|k| \leq S_{sym}$ , with the exception of  $(\tau, f \pm 1/T)$ , with  $(\tau, f)$  being the true delay and Doppler. Compared with those of aforementioned RS patterns, the 2D maximum unambiguous range of the proposed scheme around the true delay and Doppler (0,0) shows enhanced flexibility. Fig. 7(a) shows the AF of  $S_{sub} = 4$ ,  $S_{sym} = 1$ , and  $p = 1$  with three examples of designated unambiguous ranges and Fig. 7(c) presents the AF of  $S_{sub} = 4$ ,  $S_{sym} = 1$ , and  $p = 3$ .

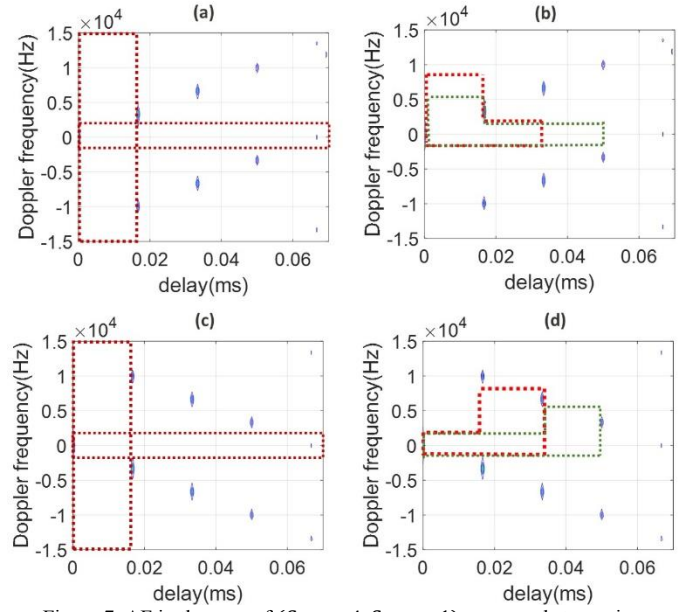


Figure 7. AF in the case of ( $S_{sub} = 4, S_{sym} = 1$ ), proposed staggering scheme, where in (a) and (b)  $p = 1$ , and in (c) and (d)  $p = 3$ .

For instance, regarding the RS pattern with  $p = 1$ , 2D maximum unambiguous 2-D range around the true delay and Doppler have following options as shown in Fig. 7(a) and (b):

- 1) Comb-sized fractional-symbol delay unambiguity:
  - a. In the case of  $S_{sym} > 1$ , time delay is from 0 to  $T_s/S_{sub}$ , and Doppler from  $I$  to  $I + 1/S_{sym}T$ , where  $I$  is a specified value with  $-1/S_{sym}T \leq I \leq 0$ .
  - b. In the case of  $S_{sym} = 1$ , time delay is from 0 to  $T/S_{sub}$ , and Doppler from  $I$  to  $I + N/S_{sym}T$ , where  $I$  is a specified value with  $-N/S_{sym}T \leq I \leq 0$  as shown in Fig. 7(a).
- 2) Full-symbol unambiguous delay extended to  $T_s$  as shown by the horizontally wider dotted red rectangle in Fig. 7(a): Doppler range is now from  $J$  to  $J + 1/S_{sym}S_{sub}T$ , where  $J$  can be specified within the range of  $-1/S_{sym}S_{sub}T \leq J \leq 0$ .
- 3) Designated unambiguous delay from 0 to  $lT_s/S_{sub}$ , where  $l = 2, \dots, S_{sub} - 1$ , as shown in Fig. 7(b): One designated 2D maximum unambiguous range is expressed as:

$$\begin{cases} J < f_d < J + \frac{S_{sub} - l + 1}{S_{sub}S_{sym}T}, & 0 < \tau < \frac{T_s}{S_{sub}} \\ J < f_d < J + \frac{1}{S_{sub}S_{sym}T}, & \frac{T_s}{S_{sub}} \leq \tau < \frac{lT_s}{S_{sub}} \end{cases}$$

where  $J$  is a specified value with  $-1/S_{sym}S_{sub}T \leq J \leq 0$ . Another choice could be:

$$\begin{cases} J - \frac{S_{sub} - l}{S_{sub}S_{sym}T} < f_d < J + \frac{1}{S_{sub}S_{sym}T}, & \frac{(l-1)T_s}{S_{sub}} \leq \tau < \frac{lT_s}{S_{sub}} \\ J < f_d < J + \frac{1}{S_{sub}S_{sym}T}, & 0 < \tau < \frac{(l-1)T_s}{S_{sub}} \end{cases}$$

where  $J$  is a specified value with  $-1/S_{sym}S_{sub}T \leq J \leq 0$ . In summary, the staggering offset sequence  $F_i = \text{mod}(p \cdot (i - 1) + \beta_1, S_{sub})$ , where  $p$  is relatively prime to  $S_{sub}$  and  $\beta_1 \in$



$\{0, 1, \dots, S_{sub} - 1\}$ , is suggested for delay-and-sum algorithms as it can be extended to more flexible 2D unambiguous range.

#### IV. EXTENDED GUARD INTERVAL FOR COMB RS

When applying OFDM to joint communication and sensing, post-FFT frequency domain sensing algorithms (e.g., 2D FFT, high-resolution algorithms [2, 7]) are conventionally limited by CP duration, which determines the maximum time delay (hence distance) that can be detected without inter-symbol interference (ISI). In this section, we will show that the frequency domain comb RS pattern with zero-power REs padded in between could extend the guard interval against ISI beyond CP such that flexibility for tuning the maximum time delay up to  $(1 - 1/S_{sub})$  of the OFDM symbol length can be achieved without ISI.

Recall CP-added OFDM time sample as defined in Eq. (5), after removing the extended guard interval against ISI (i.e., first  $(N_{cp} + lN/S_{sub})$  samples,  $l \in \{0, 1, \dots, S_{sub} - 1\}$ ), the received time sequence of the  $i$ -th OFDM symbol with a delay of  $N_\tau$  samples and a phase rotation caused by Doppler is expressed as: for  $m = 0, 1, \dots, N(S_{sub} - l)/S_{sub} - 1$ , the  $m$ -th element of the remaining time sample vector  $\mathbf{G}_l$  is

$$\begin{aligned} G_l(m) &= Z \left( \frac{Nl}{S_{sub}} + N_{cp} + m - N_\tau \right) \cdot e^{j2\pi f_D l T S_{sym}} \\ &= \sum_{k=0}^{\frac{N}{S_{sub}}} X_i(kS_{sub} + F_i) e^{\frac{j2\pi(kS_{sub} + F_i)(\frac{Nl}{S_{sub}} + m - N_\tau)}{N}} e^{j2\pi f_D l T S_{sym}}, \end{aligned} \quad (9)$$

where  $0 \leq N_\tau \leq \min(N_{cp} + Nl/S_{sub}, N)$ . To recover the non-zero REs from  $\mathbf{G}_l$ , first the receiver side should perform the following phase de-rotation procedure before FFT, that is

$$G'(m) = G_l(m) e^{-\frac{j2\pi F_i (\frac{Nl}{S_{sub}} + m)}{N}}, \quad (10)$$

where  $m = 0, 1, \dots, N(S_{sub} - l)/S_{sub} - 1$ . Then, by performing FFT on  $\mathbf{G}'$ , we obtain sequence  $\mathbf{B}$  with a length of  $N \cdot (S_{sub} - l)/S_{sub}$  and

$$B(k') = \sum_{m=0}^{\frac{(S_{sub}-l)N}{S_{sub}}-1} G'(m) e^{j\frac{-2\pi k' S_{sub} m}{(S_{sub}-l)N}}. \quad (11)$$

In Eq. (11), for  $k' \in \{(S_{sub} - l)w, w = 0, 1, \dots, N/S_{sub}\}$ , we can write

$$\begin{aligned} B(k') &= (S_{sub} - l) \cdot X_i \left( \frac{k'}{(S_{sub} - l)} S_{sub} + F_i \right) \\ &\quad \cdot e^{j2\pi f_D l T S_{sym}} e^{-\frac{j2\pi N_\tau (\frac{k'}{(S_{sub}-l)} S_{sub} + F_i)}{N}}. \end{aligned} \quad (12)$$

As for  $k' \notin (S_{sub} - l)w$ , then  $B(k') = 0$ . Then the frequency-domain sequence of the  $i$ -th RS symbol for sensing algorithm analysis (with a length of  $N - lN/S_{sub}$ ) can be re-assembled to sequence  $\mathbf{X}'_i$  with the original length of  $N$  after RS symbols of the staggering sequence  $\{F_i\}$  cycle are received. For  $B(k') \neq 0$ , then we map  $X'_i(k'S_{sub}/(S_{sub} - 1) + F_i) = B(k')$ . For other RE locations other than  $k'S_{sub}/(S_{sub} - 1) + F_i$ ,  $\mathbf{X}'_i$  will be padded zeros. Therefore,  $\mathbf{X}'_i$  can be further simplified as

$$X'_i(j) = (S_{sub} - l) \cdot X_i(j) e^{j2\pi f_D l T S_{sym}} e^{-\frac{j2\pi N_\tau j}{N}}, \quad (13)$$

where  $j = 0, 1, \dots, N - 1$ . Thus, the tunable maximum time delay without ISI is  $\min(T_{cp} + lT_s/S_{sub}, T_s)$ . Note that there is a trade-off between signal energy loss and maximum time delay with different choices of  $l$ . Larger  $l$  can support larger maximum time delay but yields lower signal energy for sensing algorithms analysis. Fig. 8 illustrates an instance of  $l = S_{sub} - 1$ , and  $S_{sub} = 4$ .

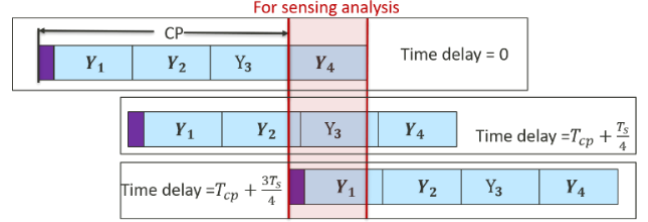


Figure 8. Sensing analysis based on  $(1/S_{sub})$ -symbol duration.

#### V. AMBIGUITY PERFORMANCE OF 2D FFT

For 2D FFT, the conclusion is similar to delay-and-sum, with the exception that side peaks appear at  $(\tau, f \pm 1/T)$ . Also, 2D FFT does not require time sequence design since the post-FFT sensing algorithm removes received frequency-domain sequence scrambling without correlation. In addition to independence from scrambling sequence properties, 2D FFT can also adopt staggered comb patterns, like their counterparts used under delay-and-sum, to eliminate side peaks of the ambiguity function produced by sensing algorithms. Based on Eq. (13), the 2D FFT algorithm performs a second FFT operation to a sequence of  $M$  descrambled post-FFT OFDM symbols  $\{\mathbf{A}_i\}_{i=0}^{M-1}$ , where

$$\begin{aligned} A_i(k_1) &= \begin{cases} \frac{X'_i(k_1)}{(S_{sub} - l)X_i(j)} = e^{j2\pi f_D l T S_{sym}} e^{-\frac{j2\pi N_\tau k_1}{N}}, & X'_i(k_1) \neq 0 \\ 0, & \text{otherwise} \end{cases} \end{aligned} \quad (14)$$

for  $k_1 = 0, 1, \dots, N - 1$ . The 2D FFT result is written as:

$$\begin{aligned} P(g, q) &= \left| \sum_{k_1=0}^{N-1} \left( \sum_{i=0}^{M-1} A_i(k_1) e^{-\frac{j2\pi q i S_{sym}}{M}} \right) e^{\frac{j2\pi g k_1}{N}} \right|^2 \\ &= \left| \sum_{k=0}^{\frac{N}{S_{sub}}-1} e^{\frac{j2\pi(g-N_\tau)kS_{sub}}{N}} \sum_{i=0}^{M-1} e^{j2\pi f_D l T S_{sym}} e^{-\frac{j2\pi q i S_{sym}}{M}} e^{\frac{j2\pi(g-N_\tau)F_i}{N}} \right|^2. \end{aligned} \quad (15)$$

For the first summation, the maximum value is obtained at  $e^{\frac{j2\pi N_\tau k S_{sub}}{N}} e^{\frac{j2\pi g k S_{sub}}{N}} = 1$ . That is, for

$$\frac{gS_{sub}}{N} - \frac{N_\tau S_{sub}}{N} = z_1 \in \mathbb{Z}, \quad (16)$$

at the 2-D FFT result there will be an AF peak at the discrete-valued time delay domain, namely  $gT_s/N$ -axis. The AF peak appears at  $\frac{gT_s}{N} = \frac{N_\tau T_s}{N} + \frac{z_1 T_s}{S_{sub}}$ . Substituting  $g = \frac{Nz_1}{S_{sub}} + N_\tau$ , terms of the second summation of Eq. (15) become

$$\sum_{i=0}^{M-1} e^{j2\pi f_D l T S_{sym}} e^{-\frac{j2\pi q i S_{sym}}{M}} e^{-\frac{j2\pi N_\tau F_i}{N}} e^{\frac{j2\pi (\frac{Nz_1}{S_{sub}} + N_\tau) F_i}{N}}$$

$$= \sum_{i=0}^{M-1} e^{j2\pi f_D i T S_{sym}} e^{-\frac{j2\pi q i S_{sym}}{M}} e^{\frac{j2\pi z_1 F_i}{S_{sub}}} \quad (17)$$

Eq. (17) is analogous to a Fourier transform of  $e^{\frac{j2\pi z_1 F_i}{S_{sub}}}$  and thus different choices of  $F_i$  yield different ambiguity peaks.

Taking the example of  $F_i$  being constant over  $i$ , terms of the summation in Eq. (17) will reach the maximum when

$$\frac{q}{MT} = f_D - \frac{z_2}{S_{sym}T}, \quad (18)$$

that is,  $e^{j2\pi f_D i T S_{sym}} e^{-\frac{j2\pi q i S_{sym}}{M}} = 1$ . The delay and Doppler ambiguities in  $\frac{q}{MT}$ -axis (Doppler domain) and  $\frac{gT_s}{N}$ -axis (delay domain) are  $\left(f_D - \frac{z_2}{S_{sym}T}\right)$  and  $\left(\frac{z_1 T_s}{S_{sub}} + \frac{N T_s}{N}\right)$ , respectively, where  $z_1 \neq 0$  and  $z_2 \neq 0$ . Fig. 9(a) shows the ambiguity performance of  $S_{sub} = 4$ ,  $S_{sym} = 1$ , and  $F_i = F_j = 0$  as one example of 2D unambiguous range. Similar to delay and sum, the maximum unambiguous delay is restricted to  $T_s/S_{sub}$ . The maximum unambiguous Doppler is smaller than delay-and-sum due to side peaks at  $(\tau, f \pm 1/T)$ .

Moreover, when  $F_i$  is not linearly changing with  $i$  (e.g., 5G PRS), the transform generates small-energy side peaks and results can be calculated numerically. Fig. 9(b) and (c) show ambiguity performances and 2D unambiguous ranges in the case of  $S_{sub} = 4$  and  $S_{sym} = 1$ , for partial PRS and PRS-like patterns, respectively.

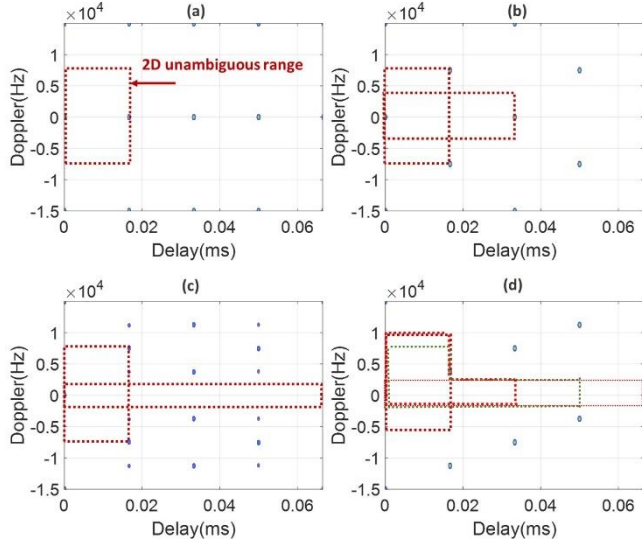


Figure 9. AF of 2D FFT with different RS patterns

When adopting proposed staggering offset, i.e.,  $F_i = \text{mod}(p \cdot (i - 1) + \beta_1, S_{sub})$ , the Fourier transform yields clean delta functions. Terms of the summation in Eq. (17) will reach the maximum when  $e^{j2\pi f_D i T S_{sym}} e^{-\frac{j2\pi q i S_{sym}}{M}} e^{\frac{j2\pi z_1 p i}{S_{sub}}} = 1$ , that is,

$f_D T S_{sym} - \frac{q S_{sym}}{M} + \frac{z_1 p}{S_{sub}} = z_2 \in \mathbb{Z}$ . This can be further written as

$$\frac{q}{MT} = f_D - \frac{z_2}{S_{sym}T} + \frac{z_1 p}{S_{sub} S_{sym}T}. \quad (19)$$

Thus, delay and Doppler ambiguities in  $q$ -axis and  $g$ -axis are  $MT \left(f_D - \frac{z_2}{S_{sym}T} + \frac{z_1 p}{S_{sub} S_{sym}T}\right)$  and  $\left(\frac{N z_1}{S_{sub}} + N \tau\right)$ , respectively, where  $z_2 \neq 0$ . Fig. 9(d) presents ambiguity performances and examples of 2D unambiguous ranges in the case of  $S_{sub} = 4$  and  $S_{sym} = 1$ , with the proposed Latin Square staggering offset. Similarly, it is also suggested for 2D FFT as an extended and more flexible 2D unambiguous range can be achieved.

## VI. CONCLUSION

In a summary, we have investigated different staggering off-sets for RS patterns with uniform symbol spacing for integrated communication and sensing systems. Moreover, we proposed an extended guard interval design for comb RS structure when using post-FFT sensing algorithms. We have studied ambiguity performances of these RS patterns using delay-and-sum and 2D FFT algorithms. In practice, one can choose an RS pattern based on the results presented in this paper and application scenarios. Overall, a form of Latin Square staggering scheme is suggested to achieve the best ambiguity performance and a more flexible choice of 2D unambiguous range under the used algorithms.

## REFERENCES

- [1] F. Liu, C. Masouros, A. P. Petropulu, H. Griffiths and L. Hanzo, "Joint Radar and Communication Design: Applications, State-of-the-Art, and the Road Ahead," in IEEE Transactions on Communications, vol. 68, no. 6, pp. 3834-3862, June 2020.
- [2] D. H. N. Nguyen and R. W. Heath, "Delay and Doppler processing for multi-target detection with IEEE 802.11 OFDM signaling," 2017 IEEE International Conference on Acoustics, Speech and Signal Processing.
- [3] P. Kumari, J. Choi, N. González-Prelcic and R. W. Heath, "IEEE 802.11ad-Based Radar: An Approach to Joint Vehicular Communication-Radar System," in IEEE Transactions on Vehicular Technology, vol. 67, no. 4, pp. 3012-3027, April 2018.
- [4] M. Braun, C. Sturm and F. K. Jondral, "Maximum likelihood speed and distance estimation for OFDM radar," 2010 IEEE Radar Conference, Arlington, VA, USA, 2010.
- [5] Q. Zhao, A. Tang and X. Wang, "Reference Signal Design and Power Optimization for Energy-Efficient 5G V2X Integrated Sensing and Communications," in IEEE Transactions on Green Communications and Networking, vol. 7, no. 1, pp. 379-392, March 2023.
- [6] Z. Wei et al., "5G PRS-Based Sensing: A Sensing Reference Signal Approach for Joint Sensing and Communication System," in IEEE Transactions on Vehicular Technology, vol. 72, no. 3, pp. 3250-3263, March 2023.
- [7] Mark Richards, Fundamentals of Radar Signal Processing, 2005.
- [8] M. Braun, M. Fuhr and F. K. Jondral, "Spectral Estimation-Based OFDM Radar Algorithms for IEEE 802.11a Signals," 2012 IEEE Vehicular Technology Conference (VTC Fall), 2012, pp. 1-5.
- [9] 3GPP TR38.211 and Chapter 24 of "5G NR: The Next Generation Wireless Access Technology, 2nd edition" by E. Dahlman, et al.